PHYSICAL REVIEW B **88**, 121404(R) (2013)

Evidence of reduced surface electron-phonon scattering in the conduction band of Bi_2Se_3 by nonequilibrium ARPES

A. Crepaldi,[1,2,*] F. Cilento,[2] B. Ressel,[2,3] C. Cacho,[4] J. C. Johannsen,[1] M. Zacchigna,[5] H. Berger,[1] Ph. Bugnon,[1] C. Grazioli,[3] I. C. E. Turcu,[4] E. Springate,[4] K. Kern,[1,6] M. Grioni,[1] and F. Parmigiani[2,7]

[1]*Institute of Condensed Matter Physics (ICMP), École Polytechnique Fédérale de Lausanne (EPFL), CH-1015 Lausanne, Switzerland*

[2]*Elettra-Sincrotrone Trieste, Strada Statale 14 km 163.5 Trieste, Italy*

[3]*University of Nova Gorica, Vipavska 11 c, 5270 Ajdovščina, Slovenia*

[4]*Central Laser Facility, STFC Rutherford Appleton Laboratory, Harwell, United Kingdom*

[5]*C.N.R.-I.O.M., Strada Statale 14 km 163.5 Trieste, Italy*

[6]*Max-Plank-Institut für Festkörperforschung, D-70569, Stuttgart, Germany*

[7]*Università degli Studi di Trieste - Via A. Valerio 2 Trieste, Italy*

(Received 12 April 2013; revised manuscript received 1 July 2013; published 16 September 2013)

The nature of the Dirac quasiparticles in topological insulators calls for a direct investigation of the electron-phonon scattering at the *surface*. By comparing time-resolved ARPES measurements of the topological insulator Bi_2Se_3 with different probing depths, we show that the relaxation dynamics of the electronic temperature of the conduction band is much slower at the surface than in the bulk. This observation suggests that surface phonons are less effective in cooling the electron gas in the conduction band.

DOI: 10.1103/PhysRevB.88.121404 PACS number(s): 78.47.jd, 73.20.−r, 78.30.−j, 79.60.−i

The scientific and technological interest on topological insulators (TIs) stems from the unusual properties of their topologically protected metallic surface states, which exhibit a linear dispersion and a characteristic spin helicity.[1–7] For the Dirac quasiparticles, elastic backscattering is forbidden by time-reversal symmetry, and transport is controlled by scattering events mediated by phonons. Attempts to measure the strength of the electron-phonon coupling in the representative TI Bi_2Se_3 by angle-resolved photoelectron spectroscopy (ARPES) have produced somewhat conflicting results. The estimated values of the dimensionless coupling constant λ vary from small ($\lambda \sim 0.08$)[8] to moderate ($\lambda \sim 0.25$).[9] Time-resolved ARPES (tr-ARPES) can tackle the problem in the time domain, complementary to the energy domain of conventional ARPES at equilibrium.[10–13] In pump-probe tr-ARPES experiments, the electrons excited by a light pulse are described by an effective Fermi-Dirac (FD) distribution. The relaxation of the electronic temperature (T_e), as well as the variation of the chemical potential (μ) that reflects photodoping of the conduction band, provide fundamental information on the deexcitation mechanisms, namely, between the conduction band (CB) and the topologically protected surface state.[12,13] In a recent experiment on Bi_2Se_3, the contribution of various phonon modes to the electronic cooling has been addressed by comparing the relaxation dynamics of the FD distribution at various sample temperatures and for different charge densities.[12]

In this work, we present a tr-ARPES investigation of the conduction band dynamics in Bi_2Se_3, where two different photon energies are exploited to vary the surface sensitivity. Standard tr-ARPES experiments, performed with laser-based sources at 6.2-eV photon energy, are rather bulk sensitive, due to the very low kinetic energy of the photoelectrons.[14] The comparison between *more* bulk-sensitive ($h\nu = 6.2$ eV; UV) and *more* surface sensitive ($h\nu = 17.5$ eV; extreme UV, EUV) measurements reveals two different relaxation dynamics for T_e in the conduction band. Namely, we observe a *freezing* of T_e to an elevated value (∼600 K) at the surface but not in the bulk, suggesting a reduced efficiency of the phonons in the electronic cooling *at the surface*.

A quantitative estimation of the photoelectron mean-free path l as a function of the photoelectron kinetic energy is challenging. In particular, it is well established that at low kinetic energies (<5 eV), the photoelectron escape depth is strongly material dependent.[15,16] An estimation of l for Bi_2Se_3 gives ∼2–3 nm at 6.2-eV photon energy.[11] This corresponds to ∼3–4 quintuple layers (QL). Whereas $l < 1$ nm at 17.5-eV photon energy, hence the escape depth is less than 1 QL.[15–17] For Bi_2Te_3,[18] Bi_2Se_3,[19–21] and other TI systems such as $PbBi_2Te_4$ and $PbBi_2Te_7$,[22] the actual models suggest that the surface-state wave function receives a large (10–20%) contribution from the second QL. This implies that the Dirac particles extend also below the surface (second and third QLs), and in principle they can be fully probed with a suitable photon energy.

The EUV tr-ARPES experiments were performed at the Artemis facility at the Central Laser Facility of the Rutherford Appleton Laboratory. The laser output at 780 nm and 1-kHz repetition rate was split in two beams. One was used to generate the tunable IR pump [here we show the results for optical excitation at 1.59 eV, and similar results were obtained by pumping at 0.95 eV (see Supplemental Material[23])], the other to generate the tunable high-harmonic (HH) EUV probe. We selected the 11th harmonic at ∼17.5 eV. The overall time resolution was 60 fs and the energy resolution was 180 meV.[23–26] The tr-ARPES experiments with 6.2-eV probe energy were performed at the T-ReX laboratory, Elettra (Trieste), with a Ti:Sa regenerative amplifier producing 780-nm laser pulses at 250-kHz repetition rate. Electrons were photoemitted by the fourth harmonics of the laser source (6.2 eV) obtained by harmonic generation in phase-matched BBO crystals. In this setup, the energy resolution was 10 meV and the temporal resolution 300 fs. Particular attention was paid in order to match the experimental conditions in the two different setups. In particular, we used

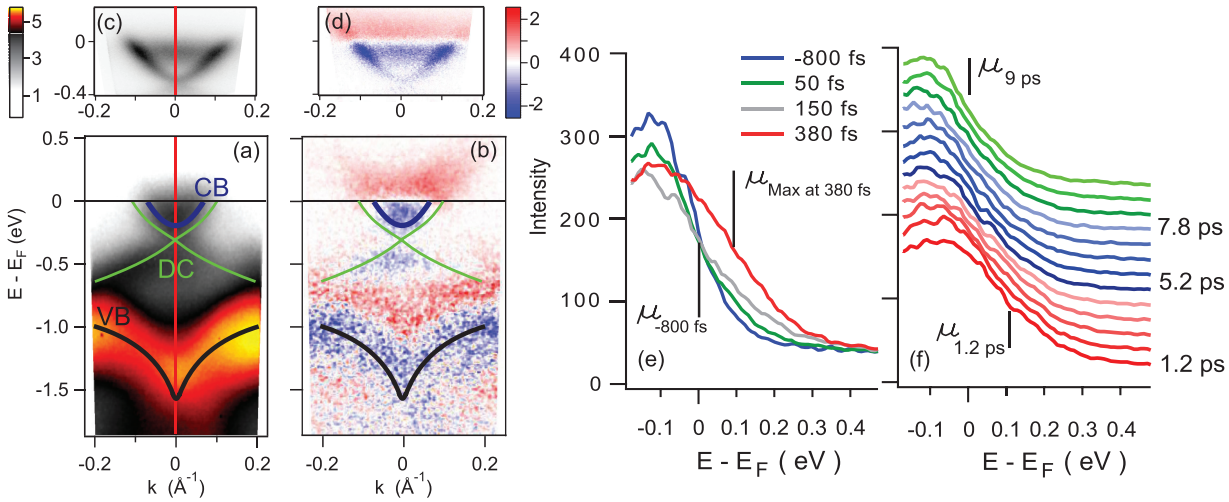

FIG. 1. (Color online) (a) ARPES image of the band structure of Bi_2Se_3 around the Γ point, measured with the surface-sensitive probe (17.5 eV) before (−500 fs) the optical excitation. Blue (green) lines outline the dispersion of the bulk (surface) states. (b) tr-ARPES image obtained as difference between the ARPES data at positive delay times (+300 fs) and the reference signal before optical excitation (−500 fs) with *s*-polarized light at 1.59 eV. (c), (d) Band structure and tr-ARPES image as panels (a), (b) measured with 6.2-eV photon energy. (e), (f) Evolution of the energy distribution curves (EDCs) taken from the ARPES data at the Γ point at selected delay times in the two temporal regions $t < 0.5$ ps (c) and $t > 1$ ps (d).

the same pump photon energy (1.59 eV) with fluence equal to 160 ± 30 $\mu J/cm^2$. The high quality *n*-doped Bi_2Se_3 samples were taken from the same batch. They were cleaved under UHV ($<5 \times 10^{-10}$ mbar) at room temperature. In each experiment, the probe beam intensity was chosen in order to make negligible space-charge effects, as witnessed by checking the energy and momentum resolution of the measured ARPES spectra.

Figure 1 compares the results obtained with 17.5- and 6.2-eV photon energies. Figure 1(a) shows as a reference the electronic states of Bi_2Se_3 around the Γ point before the optical excitation. In this and in the following figures, the binding-energy scale always refers to the Fermi-level position at negative delay time, i.e., before the optical perturbation. The Dirac cone (DC) disperses across the band gap connecting the V-shaped valence band (VB) to the conduction band (CB) and it intersects the Fermi level (E_F) at $k_F = \pm 0.1$ Å^{-1}. The data are consistent with previous ARPES experiments,[4,27,28] but the full-bandwidth preservation of the HH pulse prevents us from discerning the DC from the CB. On the other hand, the higher surface sensitivity of the EUV light enables us to investigate the out-of-equilibrium dynamics of the CB *at the surface*.

Figure 1(b) shows a tr-ARPES image obtained as a difference between the ARPES data at positive delay times (+300 fs) and the reference signal before optical excitation (−500 fs). The signal reflects a modification of the FD distribution.[10–13] Below E_F, the DC and CB drastically lose spectral weight, which is transferred above E_F. Similarly, we interpret the weak variation of intensity in the VB as an effect of thermal broadening of the valence band due to the pump pulse.[29] Figures 1(c) and 1(d) show the same as Figs. 1(a) and 1(b) but as measured with 6.2-eV photon energy. In the two data sets, the relative intensities of the surface state and the CB are different owing to matrix element effects, which provide information on the transition probability. Once the spectral features are energetically resolved, their relaxation dynamics in tr-ARPES are not affected by matrix element effects. In the present experiments, the CB is clearly resolved for both the probe photon energies, allowing us to investigate its nonequilibrium dynamics.

We now focus on the evolution of the FD distribution describing the *hot* electrons in the CB after the optical perturbation. Figures 1(e) and 1(f) show the evolution of the energy distribution curves (EDCs) at the Γ point [as indicated by the red line in Figs. 1(a) and 1(c)], integrated over a small (±0.025 Å^{-1}) wave-vector window, as a function of the delay time between the 1.59-eV pump and the 17.5-eV probe pulses. The small integration window ensures that only the dynamics of the CB is probed. The evolution of the EDCs clearly indicates the existence of two different dynamics, for $t < 0.5$ ps [Fig. 1(c)] and $t > 1$ ps [Fig. 1(d)]. At short-delay times a fast broadening is observed, which is attributed to the rapid increase of T_e. The thermal broadening of the FD function reaches its maximum at $t \sim 150$ fs [gray EDC in Fig. 1(c)]. During this fast process, the position of the chemical potential μ is unaltered. Only during the first part of the relaxation of T_e we do observe a large shift of μ [red EDC in Fig. 1(c)]. Figure 1(d) shows the evolution of the EDCs between 1.2 and 9 ps. Interestingly, while μ recovers its equilibrium value during this time interval, T_e does not, as shown by the persistent broadening of the EDCs.

A second set of data measured with 6.2-eV photons enables a direct comparison of the relaxation dynamics at the surface and in the bulk of Bi_2Se_3. Selected surface- and bulk-sensitive spectra are shown in Figs. 2(a) and 2(b), respectively. Each panel displays four EDCs measured at the Γ point at −0.8, 1.2, 6.2, and 7.8 ps delay times. The binding-energy window is the same in Figs. 2(a) and 2(b), but the kinetic energy of the photoelectrons varies by a factor ∼10 (see the top energy

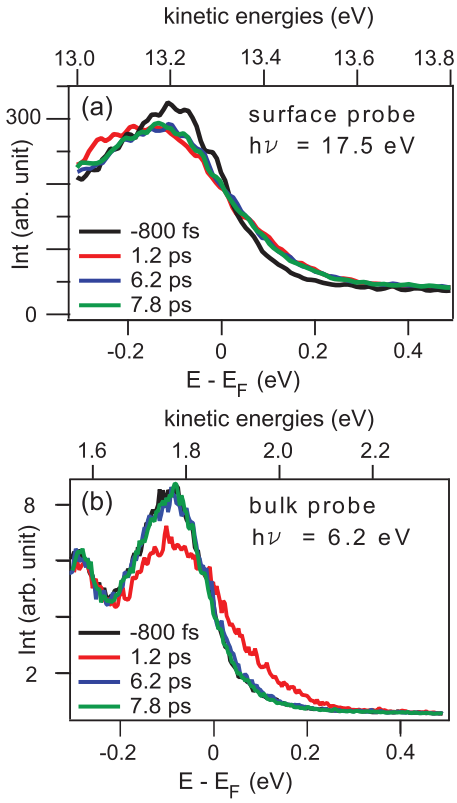

FIG. 2. (Color online) EDCs at the Γ point for different delay times: (a) surface-sensitive probe (17.5 eV); (b) bulk-sensitive probe (6.2 eV). The different broadening at negative delay time between (a) and (b) reflects the different energy resolution of the two setups. The broadening at positive delay times reflects instead an increase of T_e. In (a), the EDCs are shifted in energy to compensate the variations of μ (Fig. 1). The three EDCS at positive delays overlap, suggesting that T_e reaches a steady value. In (b), by contrast, at long-time delays ($t > 5$ ps), T_e has already relaxed back to room temperature.

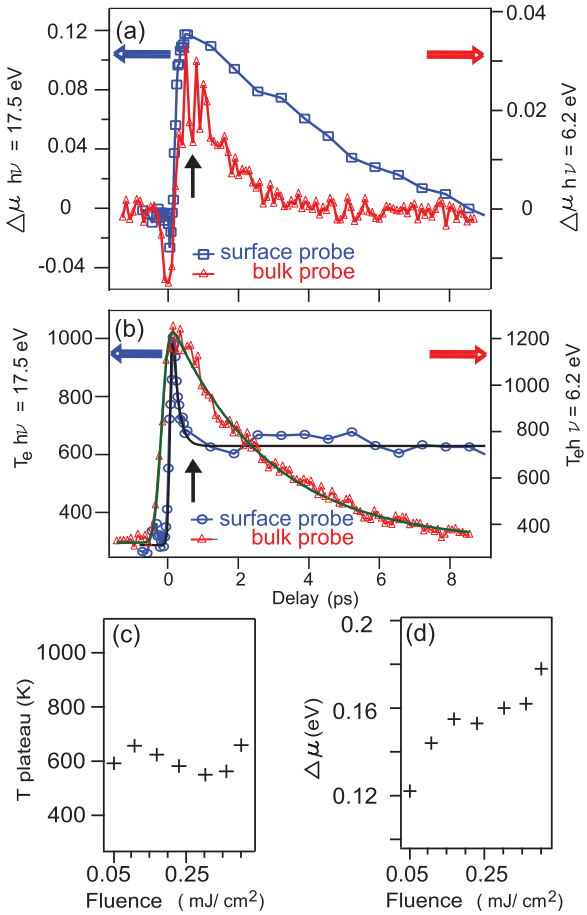

FIG. 3. (Color online) (a), (b) μ and T_e as determined by fitting a Fermi-Dirac function to the EDCs at the Γ point shown in Fig. 2. Blue (red) markers refer to 17.5-eV (6.2-eV) probe energy. In (b) the black solid line shows the best fit obtained with a single decay exponential plus a constant, with characteristic relaxation time $\tau_T = 160$ fs. At large-delay times, a steady state with $T_0 = 640$ K is achieved. The pump fluence dependence of the maximum change of μ (d) and of the plateau value of T_e (c), probed with 17.5-eV photons, is reported.

scale). The different widths of the EDCs in Figs. 2(a) and 2(b) at negative delay time are due to the different energy resolution of the two experimental setups. The broadening at positive delay times reflects the increase in T_e. In Fig. 2(a), the EDCs are rigidly shifted along the energy axis in order to compensate changes in μ. The three EDCs at positive delays overlap, thus indicating the formation of a state with large T_e, which lasts several picoseconds. By contrast, in Fig. 2(b) at the larger delay times (>5 ps), the bulk-sensitive EDCs coincide with the one at negative delay. Clearly, a nearly steady state with a high electronic temperature is generated at the surface, but not in the bulk.

We performed a quantitative analysis of the evolution of T_e and μ by fitting the leading edge of the EDCs, the so-called electronic *hot tail*, with a FD function, convolved with a Gaussian to account for the finite-energy resolution. This simple fitting procedure neglects the details contained in the analytical form of the density of states, which have been recently analyzed in other high-resolution laser tr-ARPES experiments.[12,13] Nevertheless, it provides us with a quantitative description of the peculiar effect, already visible in the raw data of Fig. 2(a). Figures 3(a) and 3(b) display the best-fit parameters for $\Delta\mu$, defined as the variation of the chemical potential before and after optical excitation, and T_e, as a function of the delay time. Blue and red markers indicate, respectively, the results for the surface- and bulk-sensitive probes. In the bulk, the relaxation of T_e is fitted with a single exponential decay with $\tau_T = 2.7$ ps, times a step function to reproduce the rise time convolved with a Gaussian to account for the temporal resolution [green line in Fig. 3(b)], in good agreement with the literature.[10,13] At the surface, a fit of T_e [black line in Fig. 2(b)] is achieved with a single exponential decay plus a constant to account for the dynamics at large-delay times. This function is multiplied by a step function to reproduce the rise time, convolved with a Gaussian to account for the temporal resolution. The high temporal resolution of the EUV setup enables us to resolve a fast relaxation with a characteristic decay time $\tau_T = 160$ fs. The underlying deexcitation mechanism is responsible also for the increase in $\Delta\mu$, resulting from the variation in the electron density in the lower-energy branch of the CB. This indicates that electrons populate the bottom of the CB

after scattering from higher-energy states, as proposed in Ref. 10.

The second dynamics observed in T_e is approximated by a constant at large-delay times, and the resulting best-fit parameter is $T_0 = 640$ K. A black arrow indicates the crossover between the two relaxation dynamics. The same delay time in Fig. 3(a) corresponds to the maximum of $\Delta\mu$. The two relaxation dynamics are unaffected by changing the pump energy to 0.95 eV. Also, at this excitation energy T_e does not relax back to its equilibrium value, but it exhibits a *plateau* at ∼550 K (see Supplemental Material[23]).

Previous bulk-sensitive tr-ARPES studies reported a characteristic relaxation time of T_e of the order of few ps (2.5 ps,[13] 1.7 ps[10]), in agreement with our bulk-sensitive probe. In all the previous investigations, such time scale was unambiguously attributed to the electron-phonon interaction. The energy deposited in the electronic bath by the pump pulse is transferred to the lattice via scattering with phonons. The characteristic relaxation time of T_e is a measure of the strength of the electron-phonon scattering in the material.[30] We interpret the long-lasting out-of-equilibrium value of T_e in the conduction band of Bi_2Se_3 as a manifestation of a reduced efficiency of the phonon scattering *at the surface*, as a mechanism to remove energy from the excited electronic bath. Interestingly, the temperature characterizing the *plateau* in Fig. 3(a) ($T_0 \sim 640$ K) is comparable to the temperature (600 K) where the cooling by optical phonons is expected to be less effective for a Dirac particle,[12] while a different electron density-dependent relaxation mechanism dominates.[12] Our data suggest that below 640 K the latter scattering process is strongly suppressed at the surface influencing the relaxation dynamics of the CB. The nature of this second scattering mechanism is still under debate and further studies are required to address the role of surface acoustic phonons. It would be of importance also to clarify whether this effect is related simply to the surface properties of the material, owing to the broken translational symmetry and the lower coordination number, or whether it reflects some more fundamental properties related to the topological protection of the Dirac particle in Bi_2Se_3. The relaxation dynamics in CB is influenced by the Dirac particles dynamics through the scattering mechanisms involving transitions among the different states, modeled by a system of rate equations as proposed by Hajlaoui *et al.*[11]

The relaxation of $\Delta\mu$ can result both from the electron-phonon scattering and from the diffusion of the photoexcited electrons, which leaves the probed region, thus contributing to recover the charge density in CB at equilibrium. The difference between the relaxation of $\Delta\mu$ at the surface and in the bulk suggests that the involved mechanisms must vary significantly as a function of the photoelectron escape depth. We observe that in the bulk, $\Delta\mu$ and T_e decay on similar time scales. The electron-phonon scattering has been proposed to be the most important contribution in the relaxation of the T_e.[12,13] Hence, these similar relaxation times suggest that the electron-phonon scattering is also the dominant mechanism governing the dynamics of $\Delta\mu$. Conversely, at the surface the electron-phonon scattering is reduced and the relaxation of $\Delta\mu$ is governed by the diffusion effects. Therefore, the relaxation becomes slower at the surface, and it can not be modeled by an exponential decay.

In our surface-sensitive experiment, we also investigated the dependence of the nonequilibrium electronic dynamics on the absorbed pump fluence, which we varied between 50 $\mu J/cm^2$ and 400 $\mu J/cm^2$ (at 1.59 eV). At the ps time scale, we observe [Fig. 3(c)] the formation of a plateau in the relaxation of T_e, which is essentially independent of the pump fluence ($T_0 \sim$ 600 K). This confirms that the persistent nonequilibrium T_e is not an artifact due to the average heating of the crystal, which is expected to scale with the adsorbed fluence. Furthermore, this observation indicates that the plateau is not an artifact due to pump-induced space-charge effects, as the measured energy broadening of the Fermi-Dirac distribution does not depend on the pump fluence. The almost linear dependence of $\Delta\mu$ on the pump fluence [Fig. 3(d)] reflects the larger density of excited charges in CB.

In summary, we have performed a probe-energy-dependent tr-ARPES study of the relaxation dynamics of the electronic temperature of the conduction band in Bi_2Se_3. The use of 6.2-eV and 17.5-eV probe energies, thanks to their different surface sensitivity, offers a unique possibility to investigate the electron-phonon scattering mechanisms *at the surface* of a TI. We observe two distinct dynamics in the relaxation of T_e at the surface. An ultrafast decrease with $\tau_T \sim 160$ fs is followed by the formation of a steady state with a value $T_0 \sim 600$ K which lasts several ps. By contrast, in the bulk, T_e relaxes back to its equilibrium value with $\tau_T \sim 2.7$ ps. The nearly steady value of T_e indicates that the electron-phonon scattering is reduced at the surface of Bi_2Se_3. It would be important to verify whether a similar reduction of the electron-phonon scattering affects also the topologically protected surface state. In fact, the surface-state wave function extends in the subsurface region, i.e., in the second QL and more weakly in the third QL. At 6.2-eV photon energy, these regions are within the primary photoelectrons probed volume. Whereas, they are only partially accessible at 17.5-eV photon energy. The possibility of a reduced electron-phonon scattering in the surface state of Bi_2Se_3 is supported by the experimental observation of a weak electron-phonon coupling ($\lambda = 0.08$) of the surface state, as recently reported by conventional surface-sensitive ARPES.[8] The reduced electronic cooling at the surface of TIs would have strong implications for applications of Bi_2Se_3 in (opto)spintronics devices. We believe that a detailed description of the phonon scattering processes at the picosecond time scale must adequately take into account the observed different behavior of the surface and the bulk of Bi_2Se_3.

We acknowledge technical support from P. Rice. Access to STCF's Artemis facility was funded by LASERLAB-EUROPE II (Grant No. 228334). This work was supported in part by the Italian Ministry of University and Research under Grants No. FIRBRBAP045JF2 and No. FIRB-RBAP06AWK3 and by the European Community Research Infrastructure Action under the FP6 Structuring the European Research Area Programme through the Integrated Infrastructure Initiative Integrating Activity on Synchrotron and Free Electron Laser Science Contract No. RII3-CT-2004-506008.

*alberto.crepaldi@elettra.eu

[1]L. Fu, C. L. Kane, and E. J. Mele, Phys. Rev. Lett. **98**, 106803 (2007).

[2]D. Hsieh, D. Qian, L. Wray, Y. Xia, Y. S. Hor, R. J. Cava, and M. Z. Hasan, Nature (London) **452**, 970 (2008).

[3]M. Z. Hasan and C. L. Kane, Rev. Mod. Phys. **82**, 3046 (2010).

[4]Y. Xia, D. Qian, D. Hsieh, L. Wray, A. Pal, H. Lin, A. Bansil, D. Grauer, Y. S. Hor, R. J. Cava *et al.*, Nat. Phys. **5**, 398 (2009).

[5]Y. L. Chen, J. G. Analytis, J.-H. Chu, Z. K. Liu, S.-K. Mo, X. L. Qi, H. J. Zhang, D. H. Lu, X. Dai, Z. Fang *et al.*, Science **325**, 178 (2009).

[6]H. Zhang, C.-X. Liu, X.-L. Qi, X. Dai, Z. Fang, and S.-C. Zhang, Nat. Phys. **5**, 438 (2009).

[7]Y. Zhao, Y. Hu, L. Liu, Y. Zhu, and H. Guo, Nano Lett. **11**, 2088 (2011).

[8]Z.-H. Pan, A. V. Fedorov, D. Gardner, Y. S. Lee, S. Chu, and T. Valla, Phys. Rev. Lett. **108**, 187001 (2012).

[9]R. C. Hatch, M. Bianchi, D. Guan, S. Bao, J. Mi, B. B. Iversen, L. Nilsson, L. Hornekær, and P. Hofmann, Phys. Rev. B **83**, 241303 (2011).

[10]J. A. Sobota, S. Yang, J. G. Analytis, Y. L. Chen, I. R. Fisher, P. S. Kirchmann, and Z.-X. Shen, Phys. Rev. Lett. **108**, 117403 (2012).

[11]M. Hajlaoui, E. Papalazarou, J. Mauchain, G. Lantz, N. Moisan, D. Boschetto, Z. Jiang, I. Miotkowski, Y. P. Chen, A. Taleb-Ibrahimi *et al.*, Nano Lett. **12**, 3532 (2012).

[12]Y. H. Wang, D. Hsieh, E. J. Sie, H. Steinberg, D. R. Gardner, Y. S. Lee, P. Jarillo-Herrero, and N. Gedik, Phys. Rev. Lett. **109**, 127401 (2012).

[13]A. Crepaldi, B. Ressel, F. Cilento, M. Zacchigna, C. Grazioli, H. Berger, P. Bugnon, K. Kern, M. Grioni, and F. Parmigiani, Phys. Rev. B **86**, 205133 (2012).

[14]M. Okawa, K. Ishizaka, H. Uchiyama, H. Tadatomo, T. Masui, S. Tajima, X.-Y. Wang, C.-T. Chen, S. Watanabe, A. Chainani *et al.*, Phys. Rev. B **79**, 144528 (2009).

[15]I. Lindau and W. Spicer, J. Electron Spectrosc. Relat. Phenom. **3**, 409 (1974).

[16]S. F. Mao, Y. G. Li, R. G. Zeng, and Z. J. Ding, J. Appl. Phys. **104**, 114907 (2008).

[17]S. Hüfner, *Photoelectron Spectroscopy: Principles and Applications* (Springer, Berlin, 1995).

[18]M. G. Vergniory, T. V. Menshchikova, S. V. Eremeev, and E. V. Chulkov, Zh. Eksp. Teor. Fiz. **95**, 230 (2012) [JETP Lett. **95**, 213 (2012)].

[19]M. Ye, S. V. Eremeev, K. Kuroda, M. Nakatake, S. Kim, Y. Yamada, E. E. Krasovskii, E. V. Chulkov, M. Arita, H. Miyahara *et al.*, arXiv:1112.5869.

[20]Z.-H. Zhu, C. N. Veenstra, G. Levy, A. Ubaldini, P. Syers, N. P. Butch, J. Paglione, M. W. Haverkort, I. S. Elfimov, and A. Damascelli, Phys. Rev. Lett. **110**, 216401 (2013).

[21]M. Bahramy, P. King, A. de la Torre, J. Chang, M. Shi, L. Patthey, G. Balakrishnan, P. Hofmann, R. Arita, N. Nagaosa *et al.*, Nat. Commun. **3**, 1159 (2012).

[22]S. V. Eremeev, G. Landolt, T. V. Menshchikova, B. Slomski, Y. M. Koroteev, Z. S. Aliev, M. B. Babanly, J. Henk, A. Ernst, L. Patthey *et al.*, Nat. Commun. **3**, 635 (2012).

[23]See Supplemental Material at http://link.aps.org/supplemental/10.1103/PhysRevB.88.121404 for the detailed description of the two experimental setups and for the data acquired at 17.5 eV by pumping the system at 0.95 eV.

[24]J. C. Petersen, S. Kaiser, N. Dean, A. Simoncig, H. Y. Liu, A. L-Cavalieri, C. Cacho, I. C. E. Turcu, E. Springate, F. Frassetto *et al.*, Phys. Rev. Lett. **107**, 177402 (2011).

[25]F. Frassetto, C. Cacho, C. A. Froud, I. C. E. Turcu, P. Villoresi, W. A. Bryan, E. Springate, and L. Poletto, Opt. Express **19**, 19169 (2011).

[26]T. Rohwer, S. Hellmann, M. Wiesenmayer, C. Cohrt, A. Stange, B. Slomski, A. Carr, Y. Liu, L. M. Avila, M. Kalläne *et al.*, Nature (London) **471**, 490 (2011).

[27]D. Hsieh, Y. Xia, D. Qian, L. Wray, J. H. Dil, F. Meier, J. Osterwalder, L. Patthey, J. G. Checkelsky, N. P. Ong *et al.*, Nature (London) **460**, 1101 (2009).

[28]M. Bianchi, R. C. Hatch, Z. Li, P. Hofmann, F. Song, J. Mi, B. B. Iversen, Z. M. A. El-Fattah, P. Löptien, L. Zhou *et al.*, ACS Nano **6**, 7009 (2012).

[29]A. Othonos, J. Appl. Phys. **83**, 1789 (1998).

[30]P. B. Allen, Phys. Rev. Lett. **59**, 1460 (1987).